Real-space renormalization group for the random-field Ising model

M. E. J. Newman, B. W. Roberts, G. T. Barkema, and J. P. Sethna
Laboratory of Atomic and Solid-State Physics, Cornell University, Ithaca, New York 14853-2501
(Received 16 June 1993; revised manuscript received 26 August 1993)

We present real-space renormalization-group (RG) calculations of the critical properties of the random-field Ising model on a cubic lattice in three dimensions. We calculate the RG flows in a two-parameter truncation of the Hamiltonian space. As predicted, the transition at finite randomness is controlled by a zero-temperature, disordered critical fixed point, and we exhibit the universal crossover trajectory from the pure Ising critical point. We extract scaling fields and critical exponents, and study the distribution of barrier heights between states as a function of length scale.

I. INTRODUCTION

The critical properties of the random-field Ising model[1,2] have been the subject of intense controversy. One of the simplest of disordered systems, the model is governed by the Hamiltonian

$$\mathcal{H} \equiv -J\sum_{\langle ij\rangle} s_i s_j - \sum_i (H + h_i)s_i, \tag{1}$$

where $s_i = \pm 1$ is an Ising spin on a cubic lattice, H is a homogeneous external field, and the variables h_i are independent Gaussianly distributed random fields of mean zero and variance σ^2. The notation $\langle ij\rangle$ indicates a sum over nearest-neighbor sites. The controversy surrounded the existence of a ferromagnetic phase transition at weak disorder in three dimensions. Supersymmetry techniques[3] and experiments by Hagen and co-workers[4] appeared to indicate that arbitrarily weak disorder would break the system up into random domains at long enough length scales. Simpler arguments given by Grinstein and Ma,[5] along with experiments by Belanger *et al.*[6] suggested that ferromagnetism persisted until a critical value of the disorder was reached. The issue was settled definitively by Imbrie and others,[7,8] who proved that the latter viewpoint was the correct one.

It was realized that the unusual experimental problems posed by the random-field model are the result of extremely slow, glassy dynamics in the system. Initial treatments of the dynamics[9] concentrated on the nonequilibrium coarsening of the domains in the ferromagnetic phase: the domain walls pin on the random fields, and as the domains grow these pinning barriers grow too. When the barriers become large compared to the temperature, thermal activation becomes ineffective and the system falls out of equilibrium without establishing long-range order. Later analyses by Bray and Moore[10] and by Fisher[11] indicated that this glassy behavior extends also to the equilibrium dynamics near the critical point. They argue that as the temperature approaches the ferromagnetic transition temperature $t = [T - T_c(\sigma)]/T_c(\sigma) \to 0$ and the correlation length $\xi \sim t^{-\nu}$ grows, the effective coarse-grained Hamiltonian flows to a zero-temperature, disordered critical fixed point. Unlike most critical points, the equilibrium energy scale $E \sim t^{-\theta\nu}$ at the correlation length becomes much larger than the temperature (violation of hyperscaling). As a result, the temperature is an irrelevant variable in the renormalization group (RG) treatment of the system. The exponent ψ determining the divergence of the energy barriers

$$B \sim t^{-\psi\nu} \tag{2}$$

is assumed to equal θ, which follows from the irrelevant eigenvalue governing the RG flow of the temperature. Instead of a competition between bond energy and thermal fluctuations, the battle at long length scales is between the bonds and the (renormalized) disorder. The dynamics, which proceeds by thermal activation with time constant $\tau \sim \exp(B/kT)$, slows down exponentially already above $T_c(\sigma)$.

We present here a real-space RG calculation which directly confirms this theoretical picture. Figure 1 previews our results: the pure Ising critical point T_c is unstable to random-field disorder, and the rescaled effective temperature and disorder flow to a disordered critical fixed point at $T = 0$, $\sigma = \sigma_c$. As well as providing a useful qualitative picture of the RG flows in the model, our method gives values for the critical exponents at the two fixed points. In addition to the simple two-parameter truncation of Hamiltonian space, we consider additional forms of disorder to (a) confirm that they correspond to irrelevant operators, and (b) improve our critical exponents. The calculation gives more precise exponents than direct methods, though our systematic errors are potentially large because of our small system size. We also calculate the distribution of energy barrier heights for our system. Combining this calculation with RG results on the scaling of temperature and random-field disorder, we show explicitly how this distribution varies with length scale.

II. THE RENORMALIZATION-GROUP METHOD

We investigate the model by a straightforward computational implementation of the real-space RG (Refs.

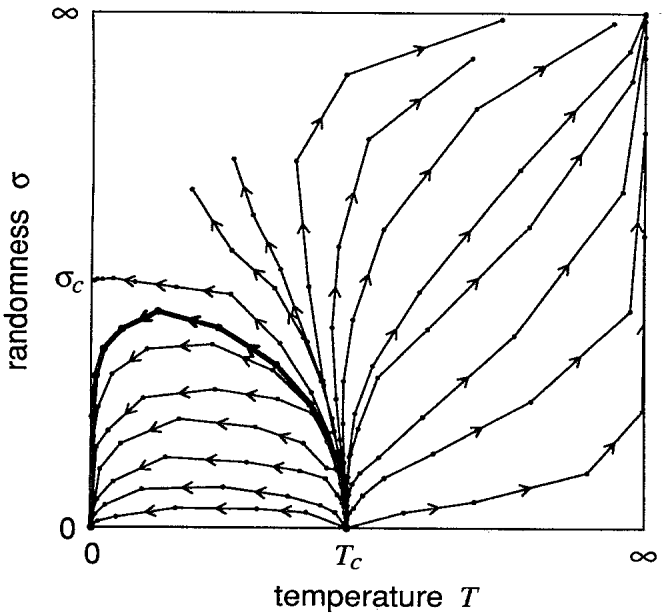

FIG. 1. Lines of RG flow through Hamiltonian space for the case of zero external field. The range $(0,\infty)$ has been mapped onto the unit square by taking hyperbolic tangents. The pure Ising fixed point is unstable to randomness: the universal critical behavior along the disordered phase boundary is determined by the fixed point at $(T=0,\sigma=\sigma_c)$. The trajectory marked with a thicker line is the one used in the calculation of the barrier height distribution, Figs. 3 and 4.

12–16) on a cubic lattice. For given values of the bond strength J, the external field H, and the variance of the random fields, the procedure is as follows.

(1) Choose random values for the variables h_i on each site of the lattice according to the Gaussian probability function

$$P_G(h,\sigma)=\frac{1}{\sqrt{2\pi}\sigma}\exp\left[-\frac{h^2}{2\sigma^2}\right]. \tag{3}$$

(2) Divide the lattice into cubic blocks of eight spins each. For each block, we define a coarse-grained spin variable s_i'.

(3) For each configuration of the coarse-grained spins, sum all the Boltzmann factors for configurations of the original lattice consistent with those spins, using the so-called "majority rule" (see Ref. 12).

(4) This defines a renormalized Hamiltonian $\mathcal{H}'$ which can be written in terms of the coarse-grained variables as

$$\mathcal{H}' \equiv -\sum_{\langle ij\rangle} J_{ij}' s_i' s_j' - \sum_i (H'+h_i')s_i' + \text{longer-range interactions}. \tag{4}$$

Once we know, numerically, the value of the renormalized Hamiltonian for each configuration of the coarse-grained variables, we can invert (4) to give the new bond strengths J_{ij}' and fields h_i' on the blocked lattice, as well as any longer-range interactions between two or more spins generated by the renormalization procedure. For example, the renormalized bond strengths are given by[12]

$$J_{ij}'=\frac{1}{4}\sum_{s_i'\ s_j'}\mathcal{H}'s_i's_j'. \tag{5}$$

(5) In the simplest case we discard all the longer-range interactions and define the renormalized bond strength to be the mean $J'=\langle J_{ij}'\rangle$ of the new bonds, the renormalized external field to be the mean $H'=\langle h_i'\rangle$ of the new fields, and the renormalized variance to be the variance of the new fields $\sigma'^2=\langle h_i'^2\rangle-\langle h_i'\rangle^2$. Later, we will consider more sophisticated versions of the RG which include higher moments in the distribution of bonds and fields than just the mean and variance considered here. These all turn out to be irrelevant operators, but their inclusion in the calculation can improve the results for the critical exponents.

To achieve good statistics we average the values of J' and σ'^2 over many different realizations of the randomness. For consistency with earlier work, we quote our results in terms of the ratios T/J and H/J, and the standard deviation of the random fields or "randomness" σ/J.

Employing the method first in two dimensions for a 4×4 system (with rules analogous to the three-dimensional ones described above) we find no nontrivial fixed points other than the pure Ising critical point.[17] We conclude that, within this approximation, there is no phase transition at finite randomness in two dimensions. This is in agreement with the findings of Imbrie,[7] Berker,[18] Bricmont and Kupiainen,[8] and others.

In three dimensions, the size of the system we can study is limited by step 3 above, in which we are required to sum over all spin configurations of the lattice. We are working on more sophisticated algorithms to speed the calculation, but for the moment we present results for a system of $2\times2\times4$ spins. This is large enough to give reasonable results, but small enough for the method to be directly applicable. Our numerical results for the RG flows, Fig. 1, are consistent with the flow diagram postulated by Bray and Moore.[10] Each point in Fig. 1 is an average over 100 different realizations of the random fields. In the regions close to the fixed points, we also performed a number of runs in which we averaged over as many as 10^6 different realizations of the randomness in order to improve the accuracy of our values for the critical exponents.

There are two nontrivial fixed points. One is the normal Ising fixed point at finite temperature and zero randomness, and the other is at zero temperature and finite randomness. This latter fixed point governs the phase transition between the paramagnetic (disordered) state and the ferromagnetic one. As predicted by Fishman and Aharony,[19] all three parameters in the problem—temperature, external field, and randomness—are relevant at the pure Ising critical fixed point. At the disordered critical fixed point only the external field and the randomness are relevant; the temperature is irrelevant. There exists a unique trajectory which leads from one critical fixed point to the other. This curve determines the crossover behavior for weakly disordered systems: far from $T_c(\sigma)$ for small σ the system will have critical fluc-

tuations given by the pure fixed point, and the growing influence of disorder is of a universal form given by this trajectory.

III. IRRELEVANT OPERATORS

The RG transformation does not actually provide us with a single renormalized value for the bond strength J', but with a distribution of strengths, which is considerably skewed from a pure Gaussian. Figure 2(a), for instance, shows a histogram of the renormalized bond-strengths J' generated by repeating the RG calculation 1 000 000 times for a set of parameters close to the disordered critical point. We can map the RG flows more accurately if we allow for this deviation from the pure Gaussian, parametrizing it by three quantities: the mean bond strength J, the standard deviation σ_J, and the skewness γ_J. In this more sophisticated calculation, we generate the bonds randomly according to the probability function

$$P_S(J,\sigma_J) = P_G(J,\sigma_J) + \frac{1}{6}\gamma_J \frac{dP_G(J,\sigma_J)}{dJ} + \frac{1}{24}K_J \frac{d^2P_G(J,\sigma_J)}{dJ^2}, \quad (6)$$

where P_G is the Gaussian probability function defined in Eq. (3). The last term in this new probability function gives the distribution a finite Kurtosis K_J as well as skewness. The Kurtosis at the disordered fixed point turns out to be negligible, but this term is kept in order to ensure that the probability function will have a positive value in the limits $J \to \pm\infty$. No higher moments were introduced in the distribution of the random fields. Figure 2(b) shows why: the distribution of the renormalized random fields close to the disordered fixed point is very close to Gaussian, so little error is introduced by assuming it to be exactly Gaussian.

We then repeat the RG calculation, this time making a histogram of the renormalized bond strengths J' over many runs to extract renormalized values σ'_J and γ'_J for the new parameters. The new parameters turn out to be irrelevant, as we would hope. And the trajectories leading away from the fixed point are again universal.

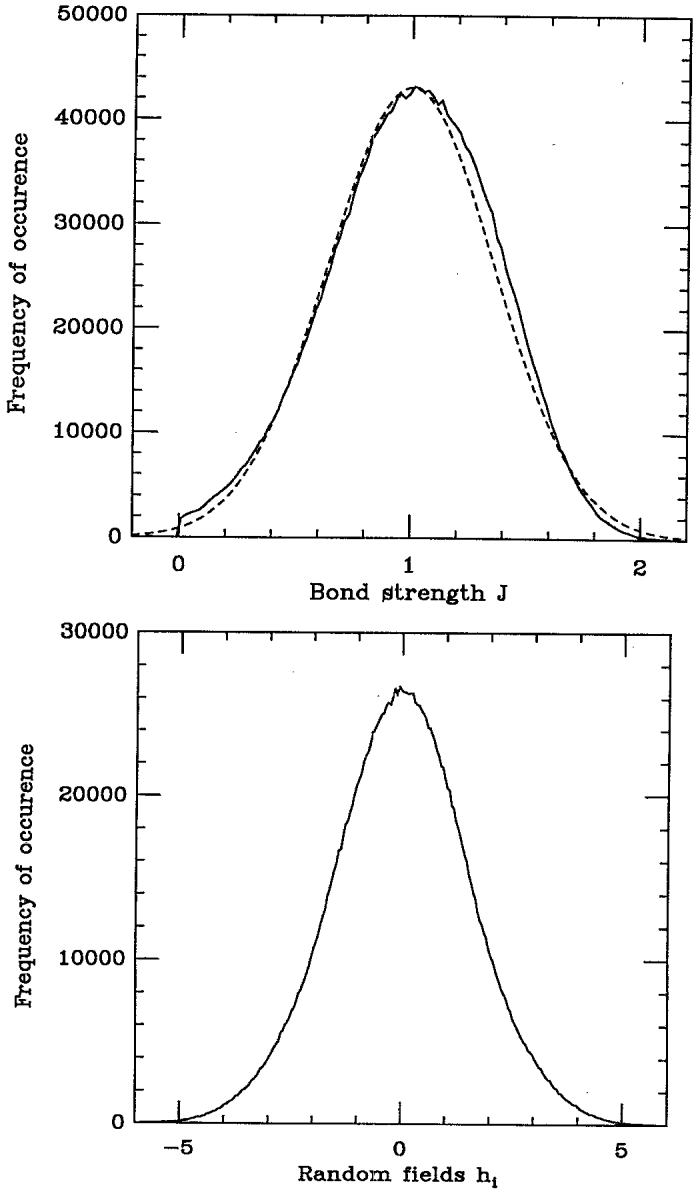

FIG. 2. (a) A histogram of the distribution of bond strengths generated by the RG procedure close to the disordered fixed point in 1 000 000 different runs. The distribution is normalized to have a mean of unity. The dashed line is a Gaussian of the same mean and standard deviation. Note that the distribution is somewhat skewed from the Gaussian. (b) The distribution of the random fields generated during the same runs. This distribution is extremely close to Gaussian.

IV. RESULTS FOR THE CRITICAL PROPERTIES

While the entire trajectory contains universal information about the critical behavior, the most commonly measured properties are the positions of the critical fixed points, and the critical exponents. Our value for the critical temperature at the pure Ising critical point is $T_c = 5.38$, which is substantially higher than the known value of 4.51, due to the small system size. Near this point, the three parameters $(T - T_c)/J$, H/J, and σ/J are expected to scale independently under the RG transformation, and our calculation confirms this. Our value for the critical randomness at the disordered critical fixed point is $\sigma_c = 1.675 \pm 0.002$. It has been conjectured[2] that near this fixed point the correct eigenvectors of the RG transformation are not the bare parameters of the problem, but are instead T/J, H/J, and the linear combination $(\sigma - \sigma_c)/J + A(T/J)$, where A is a mixing constant. We believe however that the $T = 0$ plane should be invariant under the RG transformation, and this would imply that $A = 0$ in general. Our calculation confirms this. On the other hand, we see no physical reason why T/J should be an eigenvector at the disordered critical point, and in that case the most general scaling fields for the problem would be H/J, $(\sigma - \sigma_c)/J$, and

$T/J + B(\sigma - \sigma_c)/J$. Within our numerical calculation we find that $B = 0$, but not because of any symmetry of the Hamiltonian. B is zero because the flow is asymptotically dominated by the lowest-lying states consistent with each configuration of coarse-grained spins. The argument that leads us to this result is valid for systems of any finite size, but becomes invalid in the thermodynamic limit, so it is not clear from our calculation whether B will be zero for an infinite system.

In the more sophisticated calculation, where we choose the bond strengths at random from a skewed Gaussian distribution, we find the disordered critical fixed point at $T = 0$, $\sigma = 1.55$, $\sigma_J = 0.36$, $\gamma_J = -0.20$.

Table I shows our values for the eigenvalue exponents given by linearizing the RG flows around the fixed points, together with those of previous simulations. Getting from the eigenvalue exponents to real critical exponents is straightforward. The exponents β, γ, δ, η, and ν are all defined as usual[12] along with two others; the exponent ψ, describing the divergence of the energy barriers as we approach the critical temperature, has already been defined [see Eq. (2)], and the exponent $\tilde{\eta}$ describes the dependence on q of the magnetization fluctuations at the phase boundary, for large q:

$$|\langle m_q \rangle|^2 \sim \frac{1}{q^{4-\tilde{\eta}}}. \tag{7}$$

These seven exponents are given in terms of the eigenvalue exponents by the following relations (see Table 1 of Ref. 2):

$$\begin{aligned}
\nu &= \frac{1}{y_\sigma}, \\
\beta &= \frac{d - y_H}{y_\sigma}, \\
\gamma &= \frac{2y_H - y_J - d}{y_\sigma}, \\
\eta &= 2 + d + y_J - 2y_H, \\
\delta &= \frac{y_H - y_J}{d - y_H}, \\
\tilde{\eta} &= 4 + d - 2y_H, \\
\psi &= y_J.
\end{aligned} \tag{8}$$

We have included in Table I estimates of the statistical errors. In addition to these statistical errors, we expect large systematic errors because of finite-size effects on the small lattice. Even with these systematic errors, however, our results at the important disordered fixed point are competitive with previous results.[20,21] We are extending our work to a $4\times4\times4$ system, which should allow us to include longer-range renormalized interactions and extract reliable, accurate exponents.

TABLE I. Results for the six eigenvalue exponents at the two critical fixed points. The figures in the last column are taken from Ferrenberg and Landau (Ref. 27) and Nattermann and Villain (Ref. 2).

Fixed point	Exponent	Value	Best result
Finite T	y_T	1.206	1.594 ± 0.004
fixed point	y_H	2.212	2.488 ± 0.004
	y_σ	0.509 ± 0.002	-
$T = 0$	y_σ	0.672 ± 0.005	0.9 ± 0.15
fixed point	y_H	1.88 ± 0.01	2.95 ± 0.05
	y_J	1.00 ± 0.05	1.5 ± 0.2

The eigenvalue exponents are expected to satisfy a number of different inequalities:[11,22–26] $y_H - y_J \le d/2$, $y_H \le d$, $y_J < d/2$, $y_J \le d - 1$, and $y_H - y_J/2 > d/2$. Our calculated values satisfy all of these inequalities except for the last one, where y_H is slightly less than the required value of $\frac{1}{2}(d + y_J) = 2.00$. This inequality is an expression of the fact that the magnetization fluctuations on the phase boundary between para- and ferromagnetic phases are expected to diverge in the limit $q \to 0$.[24] On the present small lattice it is not surprising then that this inequality fails. We hope that a calculation on a larger lattice would bring the value of y_H up.

V. BARRIER HEIGHT DISTRIBUTION

Our renormalization group also gives us the means to calculate the variation in the distribution of barrier heights with length scale. For the renormalized system with only two coarse-grained spins, it is a straightforward matter to calculate the distribution of barrier heights between the four possible states of the system. In the present calculation we examine the behavior of the system under single-spin-flip dynamics where the probability of a transition from state A to state B is given by the "heat-bath" formula:

$$P_{A\to B} = \frac{e_B}{e_A + e_B}, \tag{9}$$

with

$$e_i \equiv e^{-\beta E_i}. \tag{10}$$

For such a system we can define a vector $\mathbf{p} = (p_{\uparrow\uparrow}, p_{\uparrow\downarrow}, p_{\downarrow\uparrow}, p_{\downarrow\downarrow})$ giving the probability that the system will be in each of its possible states at some particular time step. The corresponding vector at the next time step is then given by $\mathbf{Mp}$, where $\mathbf{M}$ is the transfer matrix

$$\mathbf{M} \equiv \begin{pmatrix}
1 - (P_{\uparrow\uparrow\to\uparrow\downarrow} + P_{\uparrow\uparrow\to\downarrow\uparrow}) & P_{\uparrow\downarrow\to\uparrow\uparrow} & P_{\downarrow\uparrow\to\uparrow\uparrow} & 0 \\
P_{\uparrow\uparrow\to\uparrow\downarrow} & 1 - (P_{\uparrow\downarrow\to\uparrow\uparrow} + P_{\uparrow\downarrow\to\downarrow\downarrow}) & 0 & P_{\downarrow\downarrow\to\uparrow\downarrow} \\
P_{\uparrow\uparrow\to\downarrow\uparrow} & 0 & 1 - (P_{\downarrow\uparrow\to\uparrow\uparrow} + P_{\downarrow\uparrow\to\downarrow\downarrow}) & P_{\downarrow\downarrow\to\downarrow\uparrow} \\
0 & P_{\uparrow\downarrow\to\downarrow\downarrow} & P_{\downarrow\uparrow\to\downarrow\downarrow} & 1 - (P_{\downarrow\downarrow\to\uparrow\downarrow} + P_{\downarrow\downarrow\to\downarrow\uparrow})
\end{pmatrix}. \tag{11}$$

The largest eigenvalue of this matrix is unity and corresponds to the stable Boltzmann distribution of occupation

probabilities. The next largest eigenvalue is

$$\lambda = \frac{1}{2}\left(1 + \frac{|e_{\uparrow\downarrow}e_{\downarrow\uparrow} - e_{\uparrow\uparrow}e_{\downarrow\downarrow}|}{\sqrt{e_{\uparrow\uparrow}+e_{\uparrow\downarrow}}\sqrt{e_{\uparrow\uparrow}+e_{\downarrow\uparrow}}\sqrt{e_{\uparrow\downarrow}+e_{\downarrow\downarrow}}\sqrt{e_{\downarrow\uparrow}+e_{\downarrow\downarrow}}}\right). \tag{12}$$

This eigenvalue tells us about the time scale τ for the system to come to equilibrium. If the system starts with some non-Boltzmann probability vector $\mathbf{p}$ for being in each of its various states, the slowest-decaying component of the vector will be that parallel to the eigenvector corresponding to the eigenvalue λ. The time for it to decay to $1/e$ of its initial value is then given by

$$\lambda^{\tau} = \frac{1}{e}, \tag{13}$$

and this corresponds to an energy barrier B given by

$$\tau = e^{B/kT}. \tag{14}$$

Thus

$$B = -kT \ln\left[\ln\left(\frac{1}{\lambda}\right)\right]. \tag{15}$$

We calculate the barrier height distribution by repeating the calculation of this quantity for many different realizations of the random fields. Though the small size of the lattice probably means that the exact shape of the distribution is not representative of the distribution in bulk systems, the behavior of the distribution with increasing length scale, which we can extract from our RG, should be qualitatively correct. We calculate the barrier height distribution for a system with initial values J, σ of the bond strength and randomness, and also for systems along the RG trajectory that starts at this point. The successive distributions correspond to the distribution for the original system on length scales increasing by a factor of, in this case, two for each step along the trajectory. In Fig. 3 we have plotted the barrier height distributions for successive steps along one RG trajectory. This trajectory, which is indicated by the thicker line in Fig. 1, starts fractionally below T_c near the $\sigma = 0$ axis, moves along the edge of the phase boundary and lingers briefly near the disordered critical fixed point, before turning away towards the ferromagnetic fixed point at $T = 0$, $\sigma = 0$. The barriers are plotted in multiples of the bond strength at each stage, and the vicinities of the fixed points are visible in the progression to longer length scales as stationary regions in which the distribution changes little. Figure 4 shows the mean barrier height, this time with the factors of J included, as a function of length scale. Scaling near the fixed points is represented by the straight-line portions of this plot. The zero slope follows from hyperscaling; the slope 2 follows from the area of an interface. The structure at shorter length scales will probably not have an effect on experiments, since it represents mean barrier heights much less

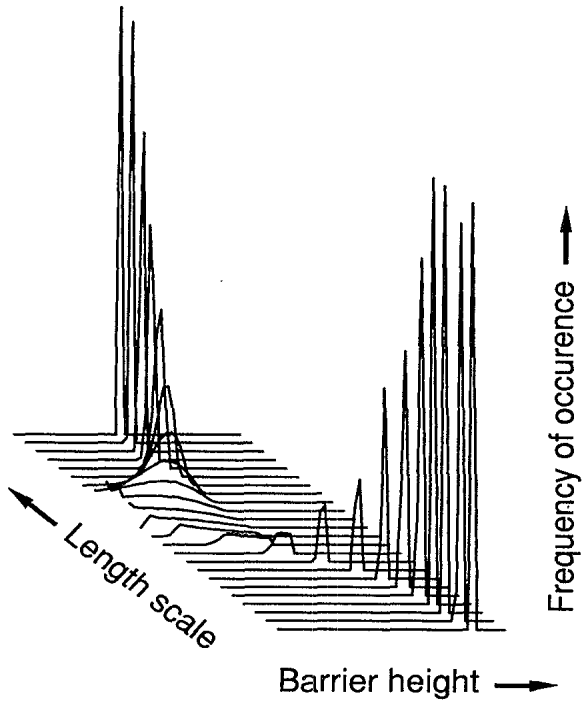

FIG. 3. The distribution of barrier heights in multiples of J for a system with small randomness, slightly below the critical temperature, shown at increasing length scales.

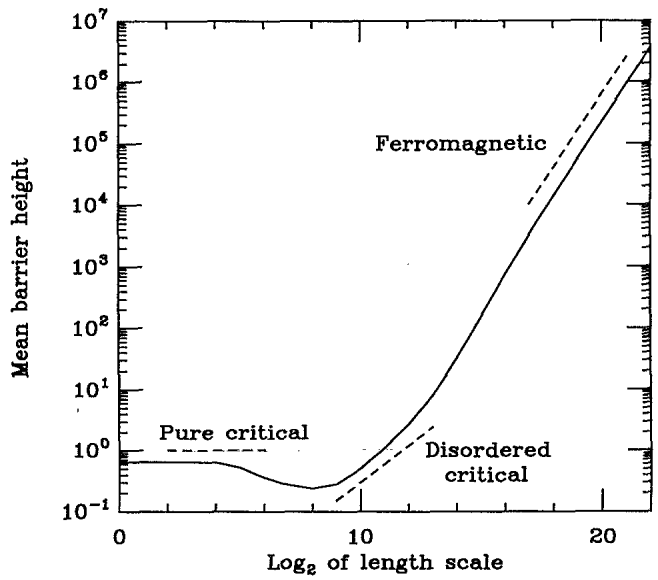

FIG. 4. The mean barrier height as a function of length scale for a system with small randomness, slightly below the critical temperature. The dotted lines indicate the expected scaling of the mean barrier height in the vicinity of the three fixed points: the slopes are zero, 1.00 ± 0.05, and two, respectively.

than kT. But the behavior at longer scales, particularly the crossover between the disordered and ferromagnetic fixed points might be measurable in an experiment that correlates the size of magnetization fluctuations (related to the length scale) with the time scale on which they occur (related to the barrier height).

VI. CONCLUSIONS

In conclusion, we provide a direct implementation of the RG for the random-field Ising model on a cubic lattice, a model whose unusual scaling behavior was the cause of substantial controversy and which now provides the best understood example of glassy dynamics. Our results for the RG flows under coarse graining confirm earlier conjectures concerning the position and nature of the fixed points. It is encouraging that the statistical errors on our exponents are much smaller than the errors generated by other techniques. If the systematic errors that arise from working on the smallest possible lattice can be reduced by going to larger lattices, the technique promises exponents of greater accuracy than those available at present. The RG also gives us a simple method for calculating the barrier height distribution as a function of length scale. The results may have experimentally measurable consequences.

ACKNOWLEDGMENTS

We would like to thank J. F. Marko for helpful suggestions. This work was partly funded by the Hertz Foundation (B.W.R.), the Science and Engineering Research Council of Great Britain (M.E.J.N.), and the NSF under Grant Nos. DMR-91-18065 (B.W.R., J.P.S.) and DMR-91-21654 (G.T.B.).

[1] D. P. Belanger and A. P. Young, J. Magn. Magn. **100**, 272 (1991).
[2] T. Nattermann and J. Villain, Phase Trans. **11**, 5 (1988).
[3] G. Parisi and N. Sourlas, Phys. Rev. Lett. **43**, 744 (1978).
[4] M. Hagen, R. A. Cowley, S. K. Satija, H. Yoshizawa, G. Shirane, R. J. Birgeneau, and H. J. Guggenheim, Phys. Rev. B **28**, 2602 (1983).
[5] G. Grinstein and S.-K. Ma, Phys. Rev. Lett. **49**, 685 (1982); Phys. Rev. B **28**, 2588 (1983).
[6] D. P. Belanger, A. R. King, V. Jaccarino, and J. L. Cardy, Phys. Rev. B **28**, 2522 (1983).
[7] J. Z. Imbrie, Phys. Rev. Lett. **53**, 1747 (1984); Commun. Math. Phys. **98**, 145 (1985).
[8] J. Bricmont and A. Kupiainen, Phys. Rev. Lett. **59**, 1829 (1987); Commun. Math. Phys. **116**, 539 (1988).
[9] J. Villain, Phys. Rev. Lett. **29**, 6389 (1984); G. Grinstein and J. F. Fernandez, Phys. Rev. B **29**, 6389 (1984).
[10] A. J. Bray and M. A. Moore, J. Phys. C **18**, L927 (1985).
[11] D. S. Fisher, Phys. Rev. Lett. **56**, 416 (1986).
[12] J. J. Binney, N. J. Dowrick, A. J. Fisher, and M. E. J. Newman, *The Theory of Critical Phenomena* (Oxford University Press, Oxford, 1992).
[13] Th. Niemeijer and J. M. J. van Leeuwen, in *Phase Transitions and Critical Phenomena,* edited by C. Domb and M. S. Green (Academic Press, London, 1976), Vol. 6.
[14] M. S. Cao and J. Machta, Phys. Rev. B **48**, 3177 (1993).
[15] S. R. McKay and A. N. Berker, J. Appl. Phys. **64**, 5785 (1988); also in *New Trends in Magnetism,* edited by M. D. Coutinho-Filho and S. M. Rezende (World Scientific, Singapore, 1990).
[16] I. Dayan, M. Schwartz, and A. P. Young, J. Phys. A **26**, 3093 (1993).
[17] M. Nauenberg and B. Nienhuis, Phys. Rev. Lett. **33**, 944 (1974).
[18] A. N. Berker, Phys. Rev. B **29**, 5243 (1984).
[19] S. Fishman and A. Aharony, J. Phys. C **12**, L729 (1979).
[20] A. T. Ogielski, Phys. Rev. Lett. **57**, 1251 (1986).
[21] H. Rieger and A. P. Young (unpublished).
[22] A. N. Berker and S. R. McKay, Phys. Rev. B **33**, 4712 (1986).
[23] M. Schwartz and A. Soffer, Phys. Rev. Lett. **55**, 2499 (1985); Phys. Rev. B **33**, 2059 (1986).
[24] J. Villain, J. Phys. (Paris) **46**, 1843 (1985).
[25] A. P. Young and M. Nauenberg, Phys. Rev. Lett. **54**, 2429 (1985).
[26] A. B. Harris, J. Phys. C **7**, 1671 (1974).
[27] A. M. Ferrenberg and D. P. Landau, Phys. Rev. B **44**, 5081 (1991).